Structure and Mechanical Properties of Thermoplastic Polyurethane, Based on Hyperbranched Polyesters

Qi Cao, Yuanli Cai, Bo Jing, Pengsheng Liu

College of Chemistry, Xiangtan University, Xiangtan, Hunan 411105, People's Republic of China

Received 15 January 2006; accepted 23 April 2006
DOI 10.1002/app.24779
Published online in Wiley InterScience (www.interscience.wiley.com).

ABSTRACT: A series of hyperbranched polyurethane (HB-PU) were synthesized using hyperbranched polyester as a precursor. Morphology of these HB-PU films was investigated using atomic force microscopy and wide-angle X-ray diffraction; it's molecular dynamics was studied by dynamic mechanical analysis. FTIR studies showed that hard segments get more aggregated to form domains in the HB-PU block copolymer as hard segment content increases. Such domain formation has a significant influence on the mechanical and thermomechanical properties of HB-PU, such as maximum stress and elongation at break. Especially, maximum stress and elongation at break increased significantly at 25 wt % of hard segment content, and the highest loss tangent was observed at the same composition. Heat of crystallization as measured by differential scanning calorimetry is also dependent on the hard segment content, and the control of hard segment content in PU block copolymers is very important in determining their physical properties. © 2006 Wiley Periodicals, Inc. J Appl Polym Sci 102: 5266–5273, 2006

Key words: hyperbranched polyurethane (HB-PU); hyperbranched polyester; atomic force microscopy; morphology; mechanical properties

INTRODUCTION

Dendritic macromolecule is one type of polymer with complex architecture that is intensively studied in most recent decade due to its special properties and potential applications, particularly in biomedical applications, catalysis, and commercial coatings.[1,2] It mainly includes dendrimers,[3] hyperbranched polymers,[4,5] and the like.[6] A variety of dendritic polymers have been reported over the past few decades,[7,8] and a large number of hyperbranched polymers have been reported based on a variety of different chemical architectures including, for example, polyesters,[9] polyethers,[10] polyamides,[11] polyphenylenes,[12] polyurethanes (PUs),[13] polysiloxysilanes,[14] and others[15]; the structure and properties of the system that depend on parameters, which characterize branched system among others, have been reported.[16,17]

PU elastomer is an essential commercial thermoplastic elastomer in biomedical and tissue engineering. During the past few decades, PUs have been widely used for biomedical applications such as vascular prostheses, endotracheal tubes, pacemaker lead wire insulation, catheters, and artificial hearts because of their excellent mechanical properties and comparatively good tissue and blood compatibility.[18–20]

Correspondence to: Q. Cao (wjcaoqi@163.com) or P. Liu (lpsh@xtu.edu.cn).

Contract grant sponsor: Science Research Foundation from Education Department of Hunan Province, People's Republic of China.

Generally, thermoplastic PU (TPU) is composed of a flexible or low melting soft segments and hydrogen-bonded rigid hard segments, the successive connection of polyol soft segments and hard segments forms an $(AB)_n$-type segmental copolymer. TPU basically shows a low-temperature T_g and a transition well above room temperature. A broad range of physical properties can be obtained by varying the molecular structure, molecular weights and distributions of the segments, and the soft/hard segment ratios. To improve the mechanical strength and bio-durability of this material for practical biomedical application, some contributions have focused on the physically crosslinked PU elastomers for long-term applications.[21–24]

Hyperbranched PU (HB-PU) was first reported by Spindler and Fréchet,[25] using thermally labile blocked isocyanates. Several dielectric relaxation studies of the linear and branched PU systems have been reported in the literature.[26–28] Roussos et al. investigated novel linear/low-branched PUs by means of dielectric techniques.[29] They examined the microphase separation in a PU consisting of hard and soft segments. Recently new PU systems with hyperbranched polymers, incorporated in a PU matrix as blends[30] or introduced in the network as a precursor,[31,32] attracted an increasing attention. They offer an opportunity for modification of the structure of the synthesized materials in a controlled way. However, thermoplastic hyperbranched PU with a chemically crosslinked structure has never been reported.

In this article, we describe the synthesis of thermoplastic hyperbranched PU, using hyperbranched polyester (Boltorn®H30, the third generation, Sweden) as a precursor. The suprastructure, morphology, and the

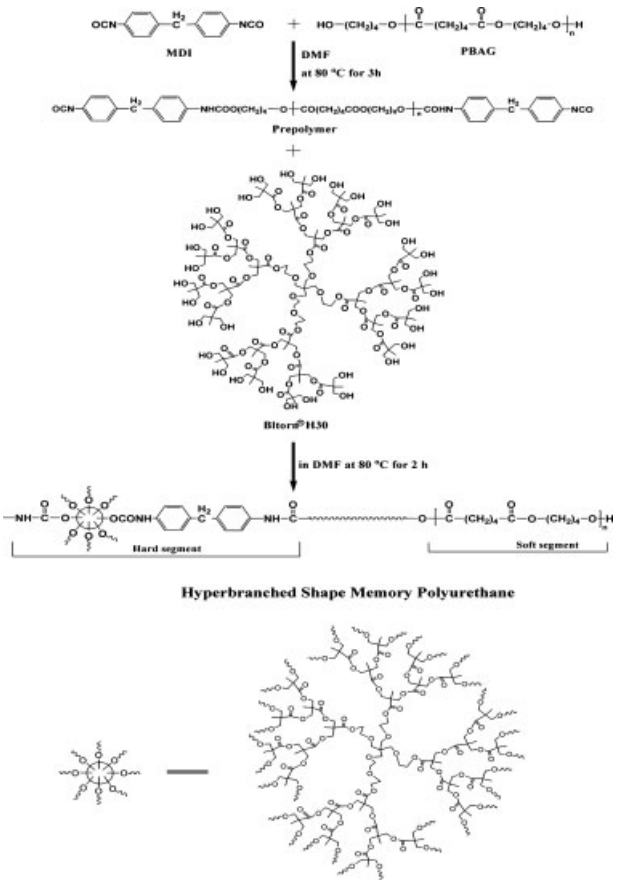

Scheme 1 Synthesis of hyperbranched polyurethane.

molecular behavior of the resulting hyperbranched TPU were investigated by wide-angle X-ray diffraction (WAXD), atomic force microscopy (AFM), and dynamic mechanical analysis.

EXPERIMENTAL SECTION

Materials

Boltorn®H30 (Third generation, M_w = 3500 g/mol, hydroxyl number equals 470–500 mg KOH/g, Sweden) was purchased from Perstorp Specialty Chemicals (Sweden), and was dried at 60°C under vacuum overnight prior to use; poly(butylene adipate)glycol (PBAG, M_w = 2000 g/mol) was purchased from Aldrich (Japan) and used without further purification; 4,4′-diphenylmethane diisocyanate (MDI) was purchased from Yantai Synthetic Leather General Factory (China), and was heated to 60°C, kept at that temperature for 2 h, and then filtered through a heated filter.

Synthesis of thermoplastic HB-PU

The synthesis route for hyperbranched PU (HB-PU) is shown in Scheme 1. The feed ratios for the resulting PU polymers are summarized in Table I. The general procedure is as follows: dehydrated PBAG and excess of MDI in 20 wt % freshly distilled DMF were charged into a 250-mL three-necked round-bottom flask equipped with magnetic stirrer immersed in a thermostatic oil-bath at 80°C under vacuum for 3 h. The chain extender of Boltorn®H30 was dissolved in dried DMF at 60°C. BoltornH30 solution was added to the flask. After stirring for 2 h, the reaction mixture was cast in glass pan and placed under vacuum at 60°C for 1 h. The solvent was removed under vacuum and further polymerized in an oven at 80°C for 24 h. The polymers were obtained as films with a thickness of 0.2–1.0 mm.

Measurements

Fourier transform infrared (FTIR) spectroscopy of the resulting TPU films was performed using the Perkin–Elmer FTIR (Model 16PC) spectrometer.

Differential scanning calorimetry (DSC) of the resulting TPU was carried out using a 2920 TA Instrument. Samples (~ 10 mg) were sealed in aluminum pans and measurements were performed in nitrogen atmosphere at a heating rate of 10°C/min in the temperature range of −50 to 150°C. In the first scanning, the sample was heated to 150°C, kept at this temperature for 5 min, and quickly cooled to −50°C. In the

TABLE I
Synthesis Parameters for HB-PU with Different Compositions

No.	Soft segment (M_n, g mol^{-1})	Chain extender	[NCO]/[OH][a]	HS content[b] (wt %)
P1	PBAG	H30	1.00	15
P2	PBAG	H30	1.00	25
P3	PBAG	H30	1.00	30
P4	PBAG	H30	1.00	35
P5	PBAG	H30	1.00	40

HS, hard segments.
[a] Feed molar ratio of isocyanate groups to hydroxyl groups.
[b] Calculated according to the feed weight ratio: HS content = $[(W_{MDI} + W_{HB30})/(W_{MDI} + W_{HB30} + W_{PBAG})] \times 100\%$.

second scanning, the sample was heated again to 150°C, and the second scan was recorded.

Thermogravimetric analysis (TGA) was carried out in Dupont TGA 2950 at a scanning rate of 20°C/min from 25 to 500°C.

Tensile test was performed following ASTM D 638 type V method, using Instron 5567 machine with a crosshead speed of 50 mm/min. The freshly prepared HB-PU specimens were immediately used for tensile test. At least five specimens were tested, and the average was plotted.

Dynamic mechanical thermal analysis (DMA) was carried out by Rheometric Scientific DMTA V device with single point bending of 2 mm thick strip at a frequency of 1 Hz and heating rate of 4°C/min from 0 to 100°C.

Wide-angle X-ray diffraction (WAXD) was employed for studying the phase morphology by using a Philip PW 1710 at 30 kV and 20 mA. WAXD studies were carried out with samples of 1 mm thickness and with Bragg's angle 2θ from 10° to 50° at the rate of 3°/min.

Tapping-mode atomic force microscopy (AFM) was used to visualize the images of TPU on a DI Nanoscope IIIa AFM; microfabricated cantilevers or silicon probes (Nanoprobes, Digital Instruments) with 125 μm long cantilevers were used at their fundamental resonance frequencies, which typically varied from 270 to 350 kHz depending on the cantilever. Cantilevers had a very small tip radius of 5–10 nm. The AFM was operated in ambient with a double vibration isolation system. Extender electronics were used to obtain height and phase information simultaneously. The lateral scan frequency was about 1.5 Hz. The images presented here are not filtered.

The samples were prepared as follows: PU was dissolved in DMF to give a 0.5 wt % diluted solution. Two microliter of the solution was deposited on a freshly cleaned silicone wafer via spin coating, followed by keeping it at 80°C in an oven for 30 min. The specimens were cooled down at room temperature prior to measurement.

RESULTS AND DISCUSSION

FTIR investigation

As shown in Figure 1, the diisocyanate (—N=C=O) band at 2250–2275 cm^{-1} was absent in the FTIR spectra of the resulting PU, indicating that this reaction was completely carried out.[33] The characteristic bands for urethane formation appear at 3320 cm^{-1} (N—H stretching); 1730 cm^{-1} (C=O stretching free from hydrogen bonding); 1710 cm^{-1} (C=O stretching with hydrogen bonding). The characteristic absorbance have been normalized by taking the sample thickness into account using the C—H absorbance at 2952 cm^{-1} as the standard.[34]

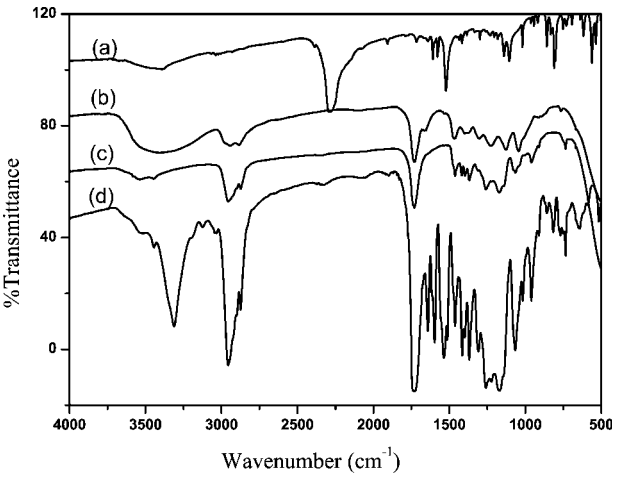

Figure 1 FTIR spectra of MDI (a), Boltorn®H30 (b), PBAG (c), and HB-PU (d).

FTIR spectroscopy has been used to characterize the hydrogen bonds in PU.[35–38] The hydrogen bonds show temperature-dependent stability as they undergo the phase mixing, reorganization, or even dissociation.[34,39] For the case of ester-based PUs, more complications arise since both the ester and urethane carbonyl groups are the potential H-bond acceptors, which consequently obscure the —C=O absorption patterns and add analysis difficult in this region. So, the overall objective of this work is to study the hydrogen bonding in the N—H stretching region (3500–3100 cm^{-1}). In this region, two major types of hydrogen bonding of ester-based PU have been identified, one is those formed by N—H of urethanes with ester carbonyl in hard segment domains, another is that of N—H of urethane with ester carbonyl in the soft segments at interphase or in soft segment domains. As shown in Figure 2 (N—H stretching spectra), HB-PU spectra exhibit the free N—H at 3444 cm^{-1} and the hydrogen-bonded N—H at 3320 and 3190 cm^{-1}, indicating that the majority of the urethane N—H has been hydrogen-bonded, the hydrogen bonded N—H peak absorbance increases and the free N—H absorbance decreases with the increase of the HB-PU hard segments. The fraction of the hydrogen-bonded N—H ($X_{b,NH}$) can be calculated according to eq. (1):

$$X_{b,\mathrm{NH}} = \frac{\text{Area (3320 cm}^{-1}\text{)} + \text{Area (3190 cm}^{-1}\text{)}}{\text{Area (3320 cm}^{-1}\text{)} + \text{Area (3190 cm}^{-1}\text{)} + K \times \text{Area (3444 cm}^{-1}\text{)}} \quad (1)$$

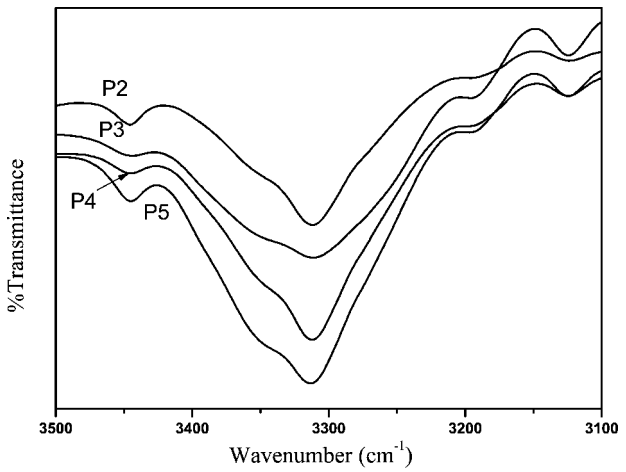

Figure 2 FTIR spectra of HB-PU with various hard segment contents in the N—H stretching region.

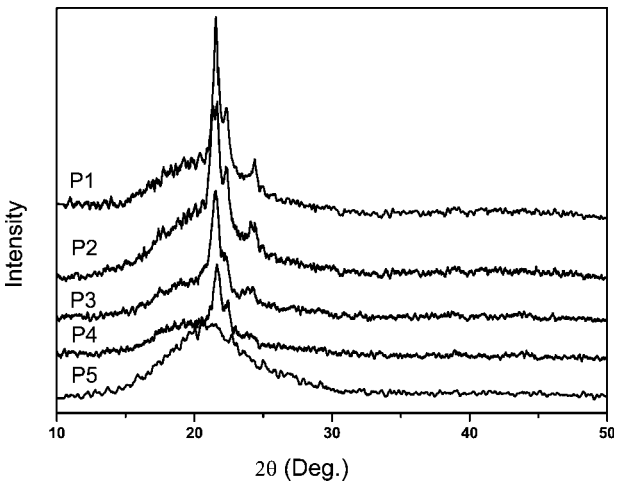

Figure 3 WAXD profiles of the HB-PU with various hard segment contents.

where $K = 3.46$,[40] and the peak areas of the free N—H spectra at 3444 cm^{-1}, hydrogen-bonded N—H at 3320 and 3190 cm^{-1} were assessed using the least-square curve fitting (Table II). It is observed that $X_{b,NH}$ increases with the hard segment contents. At room temperature, $\sim$ 90% N—H of the hard segments of a typical PU are hydrogen-bonded.[41]

Morphology

As reported in the literature,[42] the pure PBAG shows X-ray diffractions at $2\theta = 21.5^\circ$, 22°, and 24°, whereas the crystallization of PBAG segments was disturbed pronouncedly in the PBAG-based PU, due to the hindrance of hard segments.[43] As shown in Figure 3, a very diffused diffraction peak near $2\theta = 21.5^\circ$ appears for all PU of different hard segment content, and its intensity gradually decreases with increasing hard segment content. They appear to be associated with PBAG crystallization, and it means that they have the same crystal structure and unit cell type, and the crystallization of the resulting HB-PU was disturbed with the increase of hard segment content. The diffraction profiles of the HB-PU with 40 wt % hard segments finally evolved to a broad amorphous hale. These results are in good agreement with the DSC results that are to be discussed below.

The morphology of HB-PU was visualized using a tapping-mode AFM (Fig. 4). For a moderate force image, the high phase corresponds to high modulus. Therefore, the lighter phases are richer in PU, and the darker phases correspond to the polyol phase. The surface of HB-PU has phase separation of the order of 10 nm due to the hard and soft segments, similar to that observed previously.[44–46] We use a conventional interpretation of modulus-sensitive phase images at light tapping where the lighter color portions are assigned to the organized domain, i.e., the MDI-H30 hard block. The hard segment domains fill space relatively uniformly with no gross regions free of hard segment of domains. The image reveals the connected hard-segment domains. This is in general agreement with AFM images reported in the literatures.[47] Importantly, the AFM image for HB-PU with 25 wt % hard segments [Fig. 4(a,b)] shows crystallites, whereas no crystallites was observed from the image of HB-PU with 40 wt % hard segments [Fig. 4(c,d)]. This is in general agreement with the DSC and WAXD results, and the crystallites of soft segment make phase separation pronounced.

TABLE II
Least-Square Curve Fitting Results for the FTIR Spectra of N—H Region for HB-PU with Various Hard Segment Contents

	Peak area (%)			
Sample	Area 3444 cm^{-1}	Area 3320 cm^{-1}	Area 3190 cm^{-1}	$X_{b,NH}$ (%)
P2	15.1	73.3	11.6	61.90
P3	12.3	77.1	10.6	67.32
P4	11.4	78.8	9.8	69.19
P5	10.9	80.1	9.0	70.26

Thermal properties

The DSC traces of HB-PU are shown in Figure 5. The crystalline soft segment melting temperatures (T_m) are summarized in Table III. No thermotransition was observed at 100–200°C (data not shown). It is evident that the hard segment contents have influence on melting temperature of the soft segments, the melting behavior of crystallites was less pronounced as the hard segments of HB-PU increase. The melting transition of the crystalline hard segments was not observed due to more flexible backbone structure of hyper-

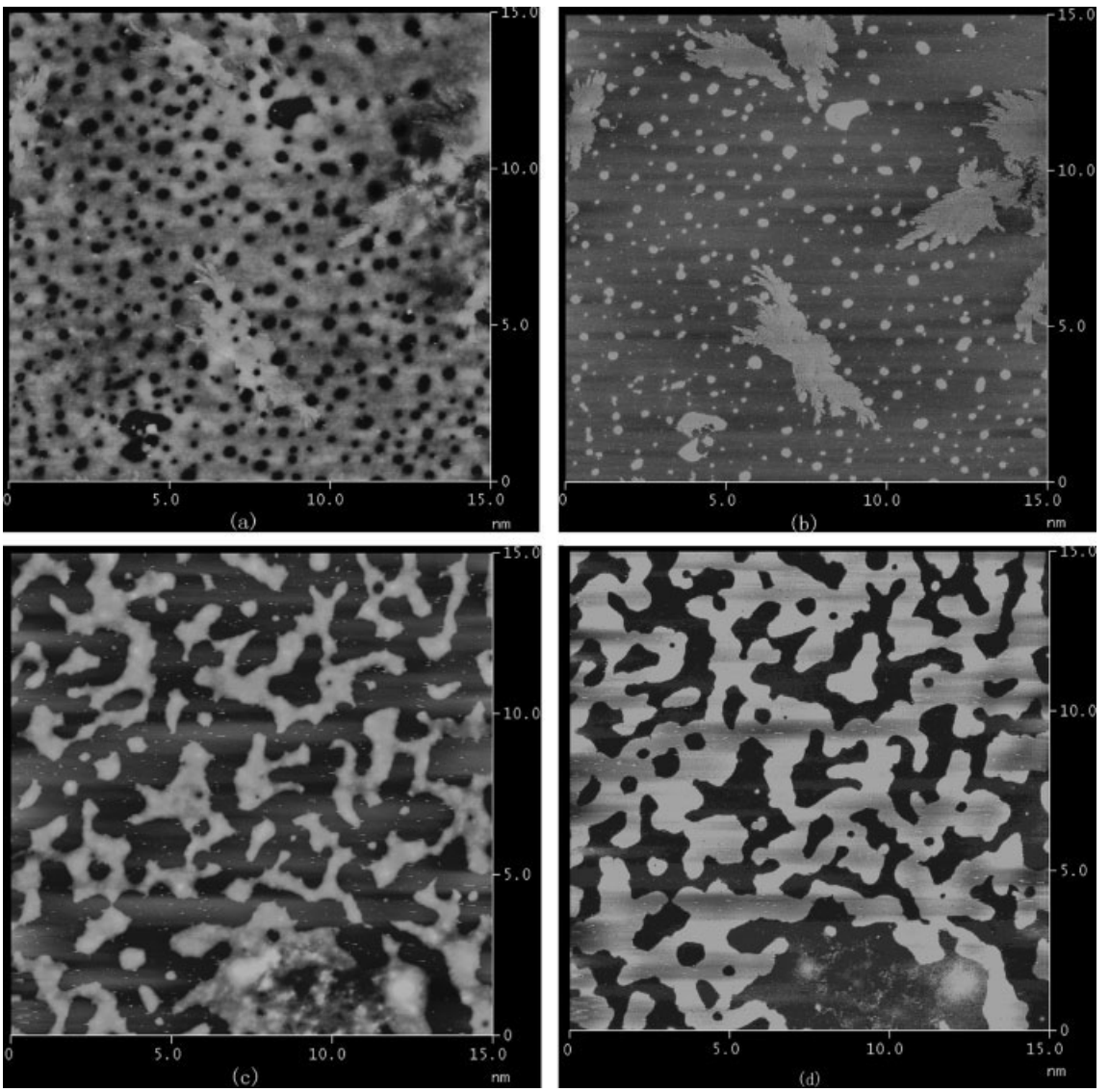

Figure 4 Tapping-mode AFM height images of HB-PU with various hard segment content: (a, b) 25 wt %; (c, d) 40 wt %; (a, c) Height; (b, d) Phase.

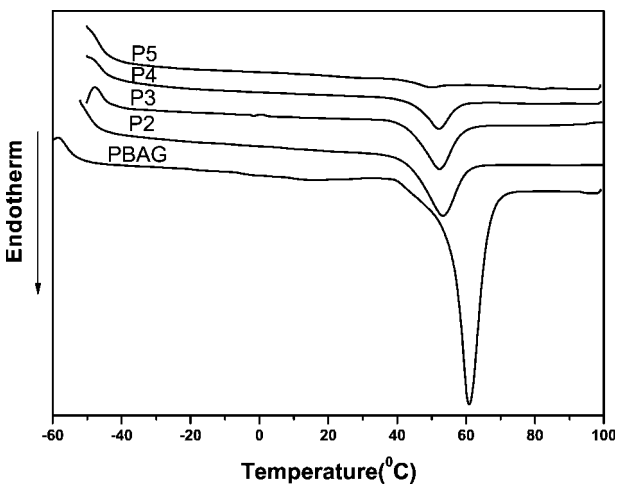

Figure 5 DSC traces for HB-PU with different hard segments: 40 wt %, 35 wt %, 30 wt %, 25 wt %, and PBAG.

branched polyester in hard segments, as compared to the conventional PU with low molecular weight dibasic alcohol chain extenders.

TABLE III
Thermal Properties of HB-PU

Material	T_m (°C)	ΔH_m (J/g)	T_1 (°C)[a]	T_2 (°C)[b]
PBAG	60.907	101.9	–	–
P1	56.187	36.55	323.2	409.7
P2	52.357	28.14	379.6	424.2
P3	51.137	26.90	365.7	412.5
P4	50.947	25.71	362.2	413.2
P5	49.265	5.88	329.7	414.7

[a] Temperature at 2% weight loss obtained from TGA curve.
[b] Peak temperature obtained from DTG curve.

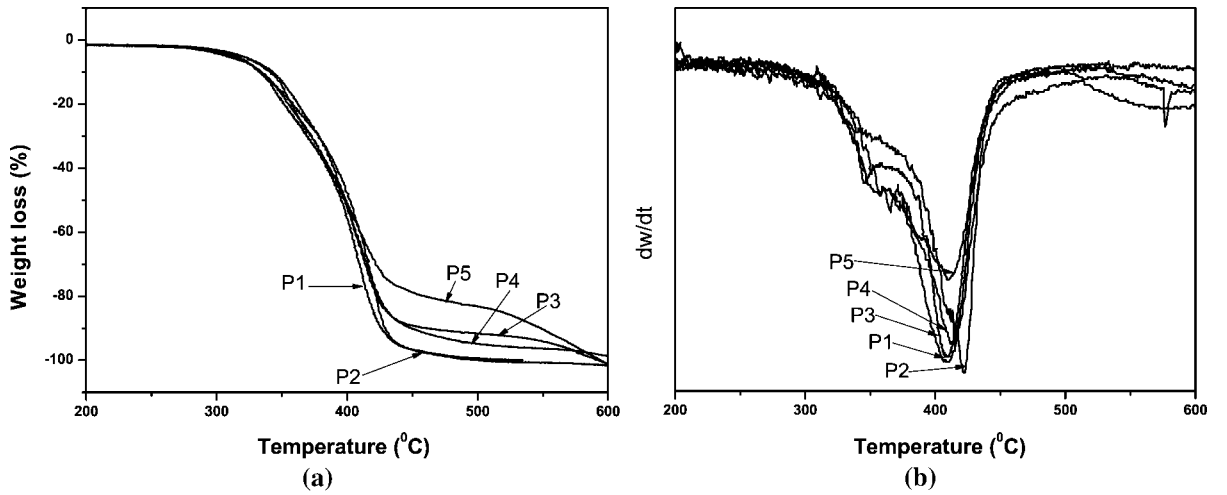

Figure 6 (a) TGA thermograms of HB-PU with various weight percent of hard segment; (b) TGA thermograms derivative curves of HB-PU with various weight percent of hard segment.

At high temperatures, e.g., above 200°C, thermoplastic PUs undergo degradation first via decomposition of urethane bonds, followed by breakage of the soft segment phase.[48,49] Such degradation process can be easily monitored by thermo gravimetric analyses (TGA), mass spectrometry, and FTIR spectrometry.[50–52]

Although the hard segment contents did not have much influence on thermal transitions, they exerted influence on thermal stability that are to be discussed below. Figure 6 presents the thermal degradation behavior of hyperbranched thermoplastic PU with various hard segment contents. The first degradation temperature (T_1) and the distinct degradation temperature (T_2) are summarized in Table III. In nitrogen, degradation is a two-step process, clearly illustrated in Figure 6(b). Results show that the thermal degradation temperatures of hyperbranched thermoplastic PU at maximum weight loss rate are in the range of 409.7–424.2°C. This indicates that increasing the hard segment contents will raise the temperature of thermal degradation. The thermal stability of this HB-PU with 25 wt % hard segments is the best among the investigated HB-PUs.

Tensile properties

Typical stress–strain diagrams of HB-PU are shown in Figure 7. Tensile properties of HB-PU block copolymers with various hard segment contents are shown in Figures 8 and 9. As shown in Figure 7, yielding and necking are observed at 15–25 wt % of hard segment, but at 40 wt % of hard segment, the PU shows neither of them, which shows a typical elastomeric character. In Figure 8, except for 25 wt %, maximum stress increases gradually up to 45 wt %, which is due to the fact that the rigid diphenylmethylene moiety coupled with hydrogen bonding and dipole–dipole interaction make the PU very difficult to stretch as higher percentage of

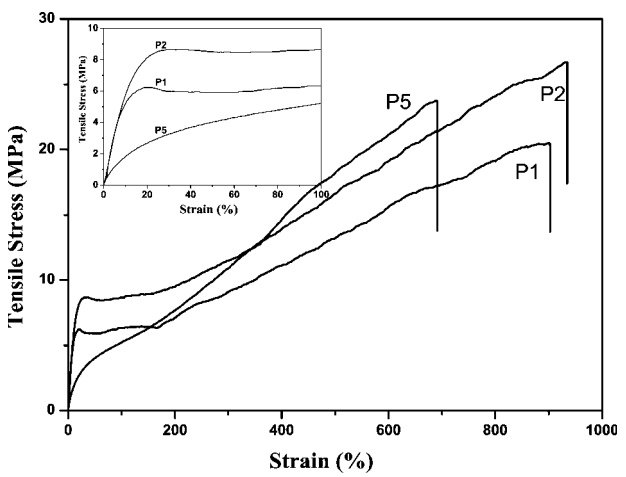

Figure 7 Stress–strain diagrams of HB-PU with various weight percent of hard segments at room temperature.

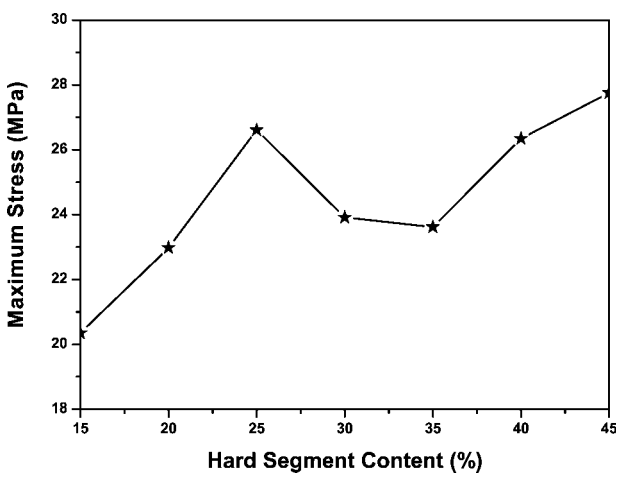

Figure 8 Tensile stress of HB-PU with various weight percent of hard segments at room temperature.

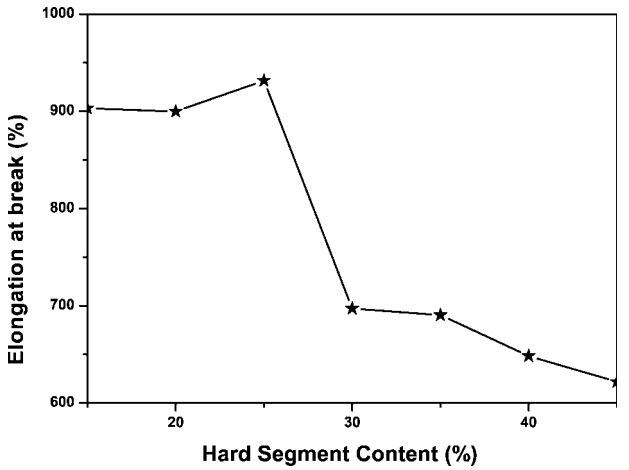

Figure 9 Percent strain at break of HB-PU with various weight percent of hard segments at room temperature.

hard segment is incorporated. In addition, physical crosslinking made by the rigid diphenylmethylene moieties also contributes to the high maximum stress with the increase of hard segment. Strains at break of HB-PU block copolymers with various hard segment contents are shown in Figure 9, where strain at break was the highest at 25 wt % of hard segment and gradually decreases with increasing hard segment content, and all PUs showed high ultimate elongation values up to 940%. At high hard segment content, the rigidity of the PU would not allow it to stretch long. Very low degree of physical crosslinking at high percentage of hard segment is responsible for the PU with low elongation.

Dynamic mechanical thermal analysis

The thermal transitions of PU were detected by DSC,[53–56] although small heat capacity of hard segment phase makes detection of glass transition temperature difficult.[57] Dynamic mechanical thermal analysis (DMA) is more sensitive than DSC and easily reveals the thermal transitions of both the soft and hard segment phases.[58,59]

Figure 10 shows the effect of different hard segments on storage modulus (E') and tan δ of HB-PU. Except for 40 wt %, storage modulus decreases with the hard segment content, and sharply changes in the T_m region, together with the slight shift of T_m to lower temperature with higher hard segment content [Fig. 10(a)]. If the soft segment PBAG could crystallize, it would show a different modulus value with each different degree of crystallization at low temperatures.[60] Hence, the soft segment of the studied samples was in the crystalline state; studies of DSC and WAXD yielded the same results. E' curve of 40 wt % HB-PU is a roughly level off in the range of 0–80°C (Fig. 10), suggesting predominantly amorphous soft segment phase of this HB-PU, which agreed with the DSC and WAXD results. In addition, the soft segmental mobility (α transition) is observed at ~ 50°C, except that tan δ curve of 40 wt % HB-PU is a roughly level off in the range of 0–80°C [Fig. 10(b)]. In Figure 10(b) is compared the loss tangent of PU block copolymers. Loss tangent for the PUs decreased with the increasing hard segment, and the highest loss tangent value of 0.65 was obtained at 25 wt % of hard segment. Damping effect at T_m is known to be dependent heavily on the hard segment content and crystallization of soft segment.[61–63] The best damping effect of PU could be expected at 25 wt % of hard segment content.

CONCLUSIONS

From FTIR spectra, HB-PU becomes more intra- or interconnected through dipole–dipole interaction, hydrogen bonding, and induced dipole–dipole interaction as the hard segment content increases. Mechanical properties of HB-PU are influenced by the hard segment content and phase separation. Low crystallinity

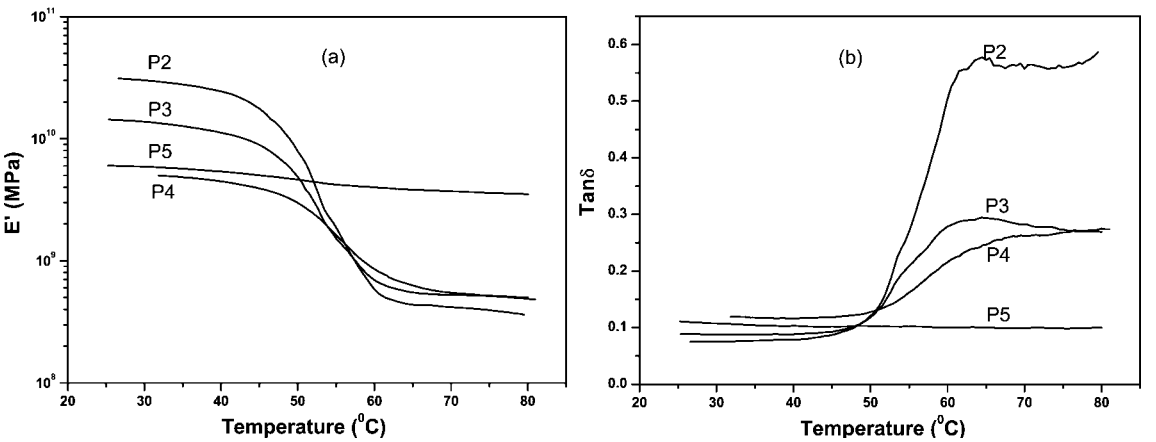

Figure 10 Storage modulus (E') and tan δ of HB-PU with various weight percent of hard segment as a function of temperature.

of soft segments decreases as the hard segment content increase. The highest loss tangent was observed for HB-PU with 25 wt % hard segments, suggesting the importance of the combination of hard segment and soft segment. Importantly, the AFM image for HB-PU with 25 wt % hard segments shows crystallites, but no crystallite was observed from the image for HB-PU with 40 wt % hard segments. This is in general agreement with the results of DSC and WAXD. Consequently, control of hard segment content in PU is very important in preparing ideal HB-PU. Further work, including modification of PU content, is underway in our laboratory.

References

1. Breton, M. P. U.S. Pat. 5,266,106 (1998).
2. Winnik, F. M. U.S. Pat. 5,098,475 (1998).
3. Tomalia, D. A.; Naylor, A. M.; Goddhard, W. A. Angew Chem Int Ed Engl 1990, 29, 138.
4. Kim, Y. H.; Webster, O. W. Macromolecules 1992, 25, 5561.
5. Inoue, K. Prog Polym Sci 2000, 25, 453.
6. Fréchet, J. M. J.; Tomalia, D. A. Dendrimers and Other Dendritic Polymers; Wiley: West Sussex, 2001.
7. Desimone, J. M. Science 1995, 269, 1060.
8. Yates, C. R.; Hayes, W. Eur Polym J 2004, 40, 1257.
9. Malmstrom, E.; Johansson, M.; Hult, A. Macromolecules 1995, 28, 1698.
10. Percec, V.; Kawasumi, M. Macromolecules 1992, 25, 3843.
11. Uhrich, K. E.; Boegeman, S.; Fréchet, J. M. J.; Turner, S. R. Polym Bull 1991, 25, 551.
12. Kim, Y. H.; Webster, O. W. Macromolecules 1992, 25, 5561.
13. Spindler, R.; Fréchet, J. M. J. Macromolecules 1993, 26, 4809.
14. Miravet, J. F.; Fréchet, J. M. J. Macromolecules 1998, 31, 3461.
15. van Benthem, R. A. T. M.; Muscat, D.; Stanssens, D. A. W. Polym Mater Sci Eng 1999, 80, 72.
16. Kim, Y. H. J Polym Sci Part A: Polym Chem 1998, 36, 1685.
17. Gao, C.; Yan, D. Prog Polym Sci 2004, 29, 183.
18. Lelah, M. D.; Cooper, S. L. Polyurethanes in Medicine; CRC Press: Boca Raton, FL 1986.
19. Planck, H.; Syre, I.; Dauner, M.; Egbers, G., Eds. Polyurethane in Biomedical Engineering II, Progress in Biomedical Engineering; Elsevier: Amsterdam, 1987.
20. Liu, Z. F.; Wu, X.; Yang, X. Y.; Liu, D. P. Chen, J.; Sun, R. M.; Liu, X. P.; Li, F. X. Biomacromolecules 2005, 6, 1713.
21. Thomas, V.; Kumari, T. V.; Jayabalan, M. Biomacromolecules 2001, 2, 588.
22. Takahara, A.; Tashita, J. I.; Kajiyama, T.; Takayangi, M.; MacKnight, W. J. Polymer 1985, 26, 978.
23. Jayabalan, M.; Lizymol, P. P.; Vinoy, T. Macromolecules—New Frontiers; Srinivasan, K. S. V., Ed.; Allied Publishers: New Delhi, India, 1998; p 617.
24. Jayabalan, M.; Lizymol, P. P.; Vinoy, T. Polym Int 2000, 49, 82.
25. Spindler, R.; Fréchet, J. M. J. Macromolecules 1993, 26, 4809.
26. Frubing, P.; Kruger, H.; Goering, H.; Gerhard-Multhaupt, R. Polymer 2002, 43, 2787.
27. Savelyev, Y. V.; Arhranovich, E. R.; Grekov, A. P.; Privalko, E. G.; Korskanov, V. V.; Shtompel, V. I.; Privalko, V. P.; Pissis, P.; Kanapitsas, A. Polymer 1998, 39, 3425.
28. Pissis, P.; Kanapitsas, A.; Savelyev, Y.V.; Arhranovich, E. R.; Privalko, E. G.; Privalko, V. P. Polymer 1998, 39, 3431.
29. Roussos, M.; Konstantopoulou, A.; Kalogeras, I. M.; Kanapitsas, A.; Pissis, P.; Savelyev, Y. V.; Vassilikou-Dova, A. e-Polym 2004, art no. 042. Available online at www.e-polymers.org.
30. Jahromi, S.; Litvinov, V.; Coussens, B. Macromolecules 2001, 34, 1013.
31. Nasar, A. S.; Jikei, M.; Kakimoto, M. Eur Polym J 2003, 39, 1201.
32. Okrasa, L.; Zigon, M.; Zagar, E.; Czech, P.; Boiteux, G. J Non-Cryst Solids 2005, 351, 2753.
33. Guelcher, S. A.; Gallagher, K. M.; Didier, J. E.; Klinedinst, D. B.; Doctor, J. S.; Goldstein, A. S.; Wilkes, G. L.; Beckman, E. J.; Hollinger, J. O. Acta Biomater 2005, 1, 471.
34. Seymour, R. W.; Estes, G. M.; Cooper, S. L. Macromolecules 1970, 3, 579.
35. Lee, H. S.; Wang, Y. K.; Hsu, S. L. Macromolecules 1987, 20, 2089.
36. Tao, H. J.; Meuse, C. W.; Yang, X.; Macknight, W. J.; Hsu, S. L. Macromolecules 1994, 27, 7146.
37. Meuse, C. W.; Yang, X.; Yang, D.; Hsu, S. L. Macromolecules 1992, 25, 925.
38. Coleman, M. M.; Lee, K. H.; Skrovanek, D. J.; Painter, P. C. Macromolecules 1986, 19, 2149.
39. Srichatrapimuk, V. W.; Cooper, S. L. J Macromol Sci Phys 1978, 15, 267.
40. Yoon, P. J.; Han, C. D. Macromolecules 2000, 33, 2171.
41. Seymour, R. W.; Cooper, S. L. Macromolecules 1973, 6, 48.
42. Lin, L. R.; Chen, L. W. J Appl Polym Sci 1999, 73, 1305.
43. Blackwell, J.; Gardner, K. H. Polymer 1979, 20, 13.
44. McLean, R. S.; Sauer, B. B. Macromolecules 1997, 30, 8314.
45. Garrett, J. T.; Siedlecki, C. A.; Runt, J. Macromolecules 2001, 34, 7066.
46. Kim, Y. S.; Lee, J. S.; Ji, Q.; McGrath, J. E. Polymer 2002, 43, 7161.
47. Wu, L.; Ryan, A. J. Macromolecules 2002, 35, 5034.
48. Yang, W. P.; Macosko, C. W.; Wellinghoff, S. T.; Yang, W. P.; Macosko, C. W.; Wellinghoff, S. T. Polymer 1986, 27, 1235.
49. Petrovic, Z. S.; Zavargo, Z.; Flynn, J. H.; Macknight, W. J. J Appl Polym Sci 1994, 51, 1087.
50. Chang, C. T.; Shen, W. S.; Chiu, Y. S. Polym Degrad Stab 1995, 49, 353.
51. Suhara, F.; Kutty, S. K. N.; Nando, G. B. Polym Degrad Stab 1998, 61, 9.
52. Lage, L. G.; Kawano, Y. J Appl Polym Sci 2001, 79, 910.
53. Sung, C. S. P.; Schneider, N. S. Macromolecules 1975, 8, 68.
54. Wang, C. B.; Cooper, S. L. Macromolecules 1983, 16, 775.
55. Miller, J. A.; Lin, S. B.; Hwang, K. K. S.; Wu, K. S.; Gibson, P. E.; Cooper, S. L. Macromolecules 1985, 18, 32.
56. Leung, L. M.; Koberstein, J. T. Macromolecules 1986, 19, 706.
57. Chen, T. K.; Chui, J. Y.; Sheih, T. S. Macromolecules 1997, 30, 5068.
58. Ng, H. N.; Allegrezza, A. E.; Seymour, R. W.; Cooper, S. L. Polymer 1973, 14, 255.
59. Ryan, A. J.; Stanford, J. L.; Still, R. H. Polymer 1991, 32, 1426.
60. Li, F.; Zhang, X.; Hou, J.; Xu, M.; Lou, X.; Ma, D.; Kim, B. K. J Appl Polym Sci 1997, 64, 1511.
61. Takahashil, T.; Hayashi, N.; Hayashi, S. J Appl Polym Sci 1996, 60, 1061.
62. Pissis, P.; Apekis, L.; Christodoulides, C.; Niaounakis, M.; Kyritsis, A.; Nedbal, J. J Polym Sci Part A: Polym Phys 1996, 34, 1529.
63. Seo, B. S.; Lee, H. S.; Jin, M. J. J Polym Sci 1997, 34, 148.